Rapid development and persistence of a massive Antarctic sea ice tongue

Stephen R. Rintoul,[1,2] Serguei Sokolov,[1,2] and Robert A. Massom[3]

Received 4 September 2007; revised 4 March 2008; accepted 28 May 2008; published 30 July 2008.

[1] An extraordinary sea ice tongue developed near 85°E over a period of 30 days in April–May 2002. The ice tongue extended to the north more than 800 km from the surrounding ice edge and covered an area greater than 200,000 km^2. Satellite measurements of ice extent and roughness characteristics demonstrate that the tongue persisted as a distinct feature throughout the winter. Remote sensing observations between 1978 and 2004 confirm that ice tongues occur frequently at this location, although the 2002 tongue was particularly pronounced. We show that ocean currents and winds conspire to favor the development of ice tongues at this location. Mean streamlines of the southern part of the Antarctic Circumpolar Current turn sharply to the north near 85°E after passing through the Princess Elisabeth Trough. The edge and northern limit of the ice tongue correspond well with the pattern of mean streamlines. Mean winds in April–May have a dominant southerly component in this location, favoring offshore advection of ice; year-to-year variability in the prominence of the tongue is largely caused by variations in the wind, with northerly (southerly) anomalies inhibiting (promoting) development of a sea ice tongue. Ice drift is strongly northward along the axis of the tongue, suggesting the feature is formed by advection of ice from the south rather than by in situ thermodynamic ice formation. The northward current and sea ice tongue at 85°E are associated with higher biomass at all trophic levels than observed elsewhere in east Antarctica.

Citation: Rintoul, S. R., S. Sokolov, and R. A. Massom (2008), Rapid development and persistence of a massive Antarctic sea ice tongue, *J. Geophys. Res.*, *113*, C07045, doi:10.1029/2007JC004541.

1. Introduction

[2] The physical processes controlling the location of the Antarctic sea ice edge, and therefore ice areal extent, remain poorly understood. Ice formation and melt, ocean currents and wind patterns all contribute to setting the configuration of the sea ice edge [*Allen and Long*, 2006; *Massom*, 1992], although complex atmosphere-ocean-ice interactions at work in the marginal ice zone [*Squire*, 1998] make a more complete understanding of factors determining ice edge location a difficult challenge. The location and nature of the sea ice edge are also of major ecological significance [*Ribic et al.*, 1991], with the marginal ice zone being a region of enhanced biological activity at all trophic levels, from phytoplankton [*Smith and Nelson*, 1986] to seabirds [*Ainley and Jacobs*, 1981; *Fraser and Ainley*, 1986], seals [*Siniff*, 1991] and whales [*de la Mare*, 1997; *Thiele and Gill*, 1999]. Variations in the location and characteristics of the ice edge may therefore affect the distribution of both predator and prey species [*Bornemann et al.*, 2000]. The dynamics of the marginal ice zone can also have a major effect on primary production and carbon export in the Southern Ocean [*Buesseler et al.*, 2003; *Savage et al.*, 1996], with important implications for the Southern Ocean carbon cycle and atmospheric CO_2 levels [*Sarmiento and Le Quéré*, 1996]. Improved understanding of the processes controlling the shape, location and evolution of the ice edge is therefore needed to interpret physical, biological and geochemical signals in the high-latitude Southern Ocean. A more complete understanding of factors determining Antarctic ice extent is also of major climatic significance, given that it is a sensitive indicator of variability and change in oceanic and atmospheric circulation patterns and a key metric in discussions of climate change [e.g., *Intergovernmental Panel on Climate Change* (*IPCC*), 2007].

[3] One approach to developing a better understanding of sea ice edge processes is to investigate the life cycle of particular ice edge anomalies. In April 2002, a spectacular sea ice promontory formed near 85°E (Figure 1). The sea ice tongue extended 800 km into the open ocean from the surrounding sea ice edge and covered an area of approximately 200,000 km^2. No features of similar scale are observed anywhere else in Antarctica in the image. While short-lived perturbations of the Antarctic sea ice edge are commonly observed as a result of advection by ocean

[1]Centre for Australian Weather and Climate Research, Hobart, Tasmania, Australia.
[2]Also at CSIRO Wealth From Oceans National Research Flagship Antarctic Climate and Ecosystems Cooperative Research Centre, North Ryde, New South Wales, Australia.
[3]Australian Antarctic Division, Antarctic Climate and Ecosystems Cooperative Research Centre, Hobart, Tasmania, Australia.

0148-0227/08/2007JC004541

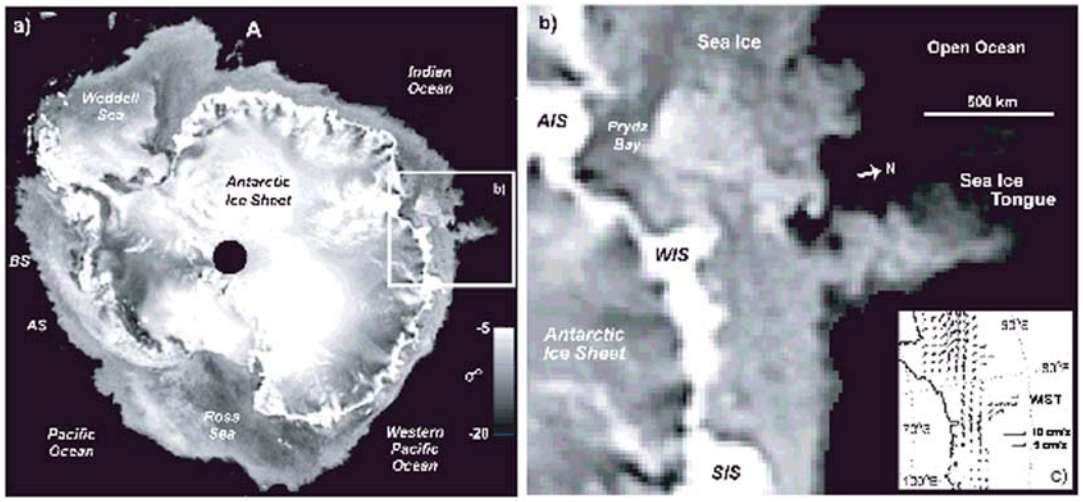

Figure 1. (a) QuikSCAT radar scatterometer enhanced-resolution sigma-0 image of Antarctica and the Southern Ocean from 30 May 2002. BS, Bellingshausen Sea; AS, Amundsen Sea. An ephemeral ice edge feature in the Weddell Sea is marked "A." (b) An expanded view of the region bounded by the white box in Figure 1a, showing the WIST. AIS, Amery Ice Shelf; WIS, West Ice Shelf; SIS, Shackleton Ice Shelf. (c) Weekly average satellite-derived sea ice motion vector data (Polar Pathfinder data set), 20–27 May 2002. Imagery courtesy of the BYU Center for Remote Sensing and NASA (QuikSCAT) and NSIDC (ice motion).

eddies or atmospheric storms [*Allen and Long*, 2006], the ice tongue at 85°E is set apart by virtue of its meridional and zonal extent and persistence. As shown in Figure 2 and discussed below, the ice tongue persisted throughout the winter. An example of a comparatively short-lived ice edge anomaly is marked A in Figure 1a showing a large band of ice that has peeled away from the main pack in the Weddell Sea. This feature then disintegrated within a few days, unlike the large tongue at 85°E which maintained its coherence throughout the entire ice season.

[4] Here we aim to develop a better understanding of the physical processes determining the location and characteristics of the sea ice edge by examining the development of the large sea ice tongue at 85°E, hitherto referred to as the West Ice Shelf sea ice Tongue (WIST). We first describe the seasonal evolution of the well-developed feature observed in 2002. Satellite data from 1978 to 2004 demonstrate that similar tongues occur in many but not all years, although the WIST was particularly prominent in 2002. Analysis of ice drift, ocean currents and winds suggests the tongue is formed primarily by advection of ice from the south rather than by local thermodynamic ice formation. Large sea ice tongues form near 85°E because both the regional ocean currents and winds in early winter favor offshore transport of sea ice in a narrow band of longitudes. Finally, we assess the impact of the WIST on the seasonal evolution of the broader sea ice pack and on the distribution of biological productivity. The life history of the WIST provides an illustration of the influence of large-scale ocean and atmosphere circulation patterns on the development of the sea ice edge and extent.

2. Data

[5] Information on the detailed structure of the WIST is obtained from enhanced-resolution sigma-0 imagery from the SeaWinds 13.4 GHz (Ku-band) radar scatterometer onboard the QuikSCAT satellite [*Early and Long*, 2001], distributed by NASA's Scatterometer Climate Record Pathfinder. The nominal pixel dimension is 4.45 km. Sea ice concentration data from the Nimbus-7 Scanning Multichannel Microwave Radiometer (SMMR) and Defense Meteorological Satellite Program (DMSP) Special Sensor Microwave/Imager (SSM/I) were obtained from the National Snow and Ice Data Center (NSIDC) [*Cavalieri et al.*, 2006]. We used daily and monthly averaged data at a grid cell size of 25 × 25 km (the daily data cover the period 1997–2004; monthly data span the period 1978–2004). Daily sea ice motion vector data, computed from NOAA Advanced Very high-Resolution Radiometer (AVHRR), SMMR and SSM/I data, were obtained from the Polar Pathfinder data set at the NSIDC [*Fowler*, 2003].

[6] To map Southern Ocean currents, we constructed absolute sea surface height fields by adding the CLS/AVISO "Mean Sea Level Anomaly" (MSLA) [*Le Traon et al.*, 1998] to the mean surface dynamic height (relative to 2500 dbar) from the WOCE (World Ocean Circulation Experiment) global hydrographic climatology [*Gouretski and Koltermann*, 2004].

[7] Atmospheric forcing patterns are examined using NCEP/NCAR Global Atmospheric Reanalysis monthly mean fields [*Kalnay et al.*, 1996], which were complemented by QuikSCAT winds after 1999 obtained from the NASA Jet Propulsion Laboratory (JPL). Bathymetry data is from the ETOPO5 digital elevation data set from the National Geophysical Data Center.

[8] Surface chlorophyll concentrations derived from satellite ocean color measurements are used to examine phytoplankton blooms in the region. The SeaWiFS data used in this study cover the period from October 1997 to December 2005. Eight day mean level 3 standard mapped images of chlorophyll on a global 9 km equidistant cylindrical grid

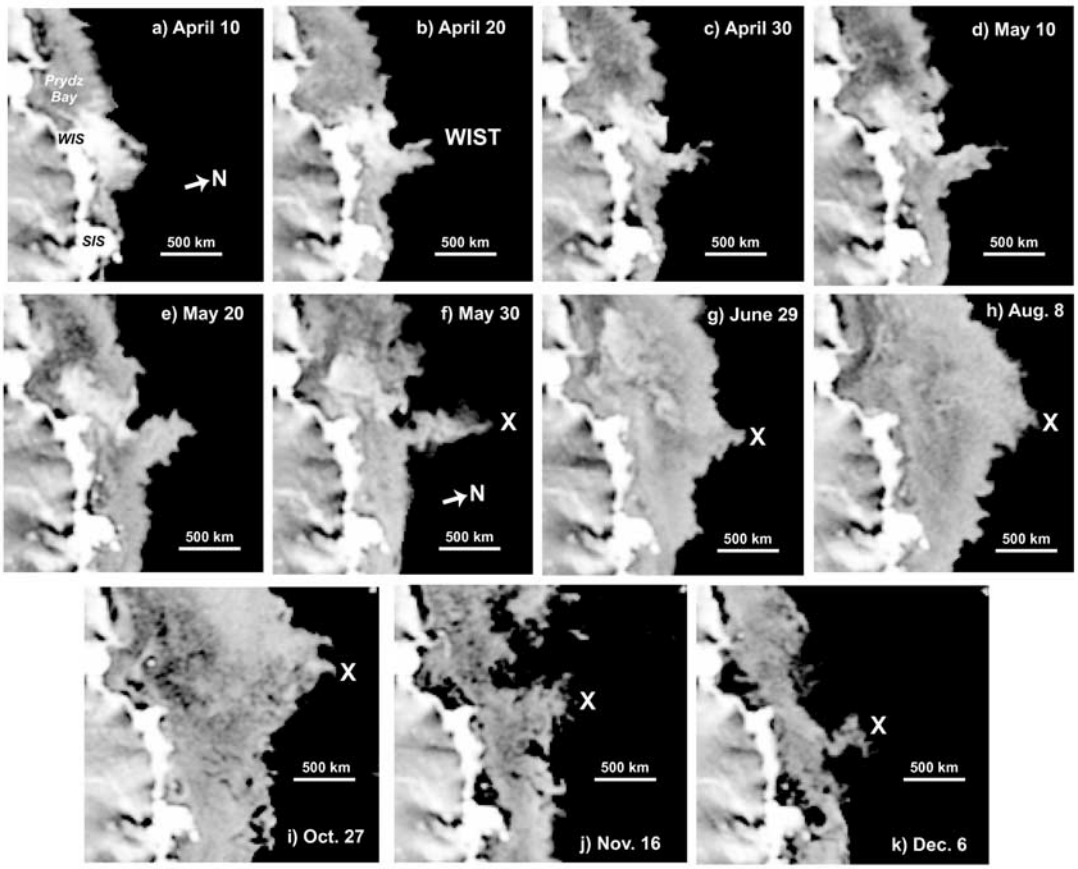

Figure 2. (a–k) Time series of QuikSCAT enhanced-resolution sigma-0 images of sector 60–100°E showing the evolution of WIST from 10 April to 6 December 2002. "X" indicates the tip of the WIST. WIS, West Ice Shelf; SIS, Shackleton Ice Shelf. Imagery courtesy of the BYU Center for Remote Sensing and NASA.

from SeaWiFS were obtained from the Distributed Active Archive Centre at the NASA Goddard Space Flight Center [*McClain et al.*, 1998].

3. Results

3.1. Evolution of the WIST in 2002

[9] Figure 2 shows a sequence of images between 10 April and 6 December 2002 illustrating the life cycle of the WIST. The ice edge begins to bulge near 85°E in early April. Within a few weeks, a distinct tongue forms roughly perpendicular to the surrounding ice edge. After one month (by 10 May), the tip of the tongue already extends more than 500 km north of the surrounding pack. The feature attains its maximum extent as a distinct entity in late May to early June, at which time it is roughly 800 km long by 300 km wide. As the sea ice growth season continues, the ice edge to the east and west advances to enclose the tongue by early August. Although the tongue is no longer a separate entity after August, the maximum meridional extent of the sea ice pack continues to be found in the vicinity of the WIST until the end of the ice growth season in late October. The tongue itself remains distinguishable in QuikSCAT imagery in the same location throughout winter, by virtue of its distinct radar backscatter signature compared to that of the surrounding pack. Radar backscatter at 13.4 GHz is highly sensitive to ice morphology and provides information on ice deformation, surface roughness and type [*Drinkwater*, 1998; *Lubin and Massom*, 2006; *Remund et al.*, 2000]. When the pack retreats toward the continent in the melt season (early November onward), the WIST re-emerges as the surrounding ice decays first (Figures 2j–2k).

[10] The presence of such a massive ice edge anomaly in 2002 raises a number of questions. Was the 2002 event a one-off occurrence, or are similar features observed in other years? What processes contributed to the formation of such a large, persistent ice edge anomaly, and why did the tongue form in this location? For example, is the WIST formed by in situ (thermodynamic) ice formation or by advection of ice formed elsewhere? What influence does the existence of a large ice tongue have on the winter and spring extent of sea ice in the surrounding region? Finally, does the existence of a large ice tongue influence the ecology of the region?

3.2. Is the WIST Present in Other Years?

[11] The seasonal development of the sea ice extent between 30°E and 150°E is illustrated by maps of the monthly mean ice edge in Figure 3. Between January and March, sea ice is limited to the continental shelf and the ice edge closely follows the configuration of the shelf. As air

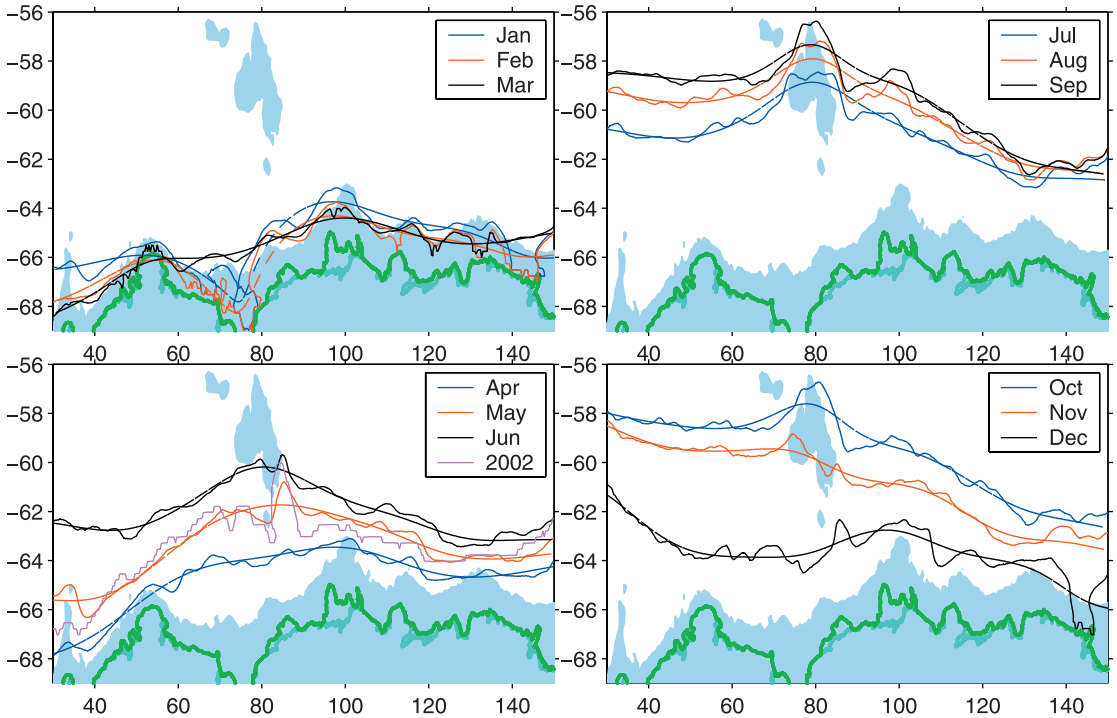

Figure 3. The monthly mean ice edge derived from sea ice concentration images from 1978 to 2004. The solid line indicates the monthly mean ice edge; the dashed line is the ice edge smoothed over a 1000-km scale. The curve labeled 2002 is the mean sea ice edge observed in May 2002. Depths shallower than 2000 m are shaded. High-resolution coastline and ice grounding line using the MODIS MOA image map [*Haran et al.*, 2006] are shown by bold solid green and cyan lines, respectively.

temperatures drop in April, sea ice begins to form and the ice edge moves to the north. At this time, the ice edge is relatively smooth, with no significant deviations from the regional-mean ice edge (indicated by the dashed lines in Figure 3, representing the ice edge smoothed over a 1000-km length scale). In May, a large ice tongue extends to the north, centered on 85°E. The fact that the feature is so distinct, even in the 26-year average, suggests that significant ice tongues form frequently in this location. The mean ice edge for May 2002 is also plotted in Figure 3c, showing the particularly large feature observed in that year and in the same location as the tongue in the long-term mean for May. By June, the ice edge on either side of the tongue has expanded northward, making the feature less distinct but still visible. As the sea ice growth season continues, the ice edge forms a bulge to the north over the relatively shallow topography (shallowest depths <1500 m) of the southern Kerguelen Plateau. As the sea ice edge retreats after reaching its maximum extent in September, there is a hint that the tongue at 85°E reappears in December, as observed in the time sequence of satellite images from 2002 shown in Figure 2.

[12] To provide a more quantitative assessment of the tendency for significant ice edge anomalies to develop in this region, we calculate the anomaly in the length of the ice edge relative to the regionally smoothed ice edge, using a smoothing scale of 1000 km. Ice edge anomalies were calculated for each month from sea ice images between 1978 and 2004 and averaged in 5 degree longitude bins (Figure 4). Ice edge length anomalies reach a strong peak near 85°E, suggesting that significant deviations from the regionally smoothed ice edge are a common feature at this location. No similar features are seen at other longitudes between 30°E and 140°E.

[13] The seasonal development of the WIST is illustrated by plotting the difference between the northernmost ice edge observed between 80°E and 90°E and the latitude of the ice edge at each longitude as a function of time through the year (Figure 5). In this representation, a purely zonal ice edge would correspond to values of zero at each longitude; a well-defined tongue would result in a band of longitudes with values near zero, flanked by larger (negative) values. A distinct tongue becomes prominent in May centered on 85°E (the orange values > −0.3°), flanked on either side by regions where the sea ice edge is more than two degrees further south (blue regions in Figure 5). During the remainder of the growth season, the ice advances on either side of the tongue (more rapidly on the western side), making a distinct tongue no longer visible in ice concentration images when the ice reaches its maximum extent in September–October. During the melt season (early November onward), the ice retreats more rapidly on either side of the WIST, causing the re-emergence of the tongue. Throughout the year, the WIST is found in a narrow band of longitude centered on 85°E.

[14] While Figures 3–5 confirm that a sea ice tongue is a recurrent feature at 85°E, the magnitude of the ice edge anomaly varies from year to year. Figure 6 shows a 26-year time series of the RMS ice edge length anomaly in May for the WIST (80°–85°E). In all years, there is a peak in the

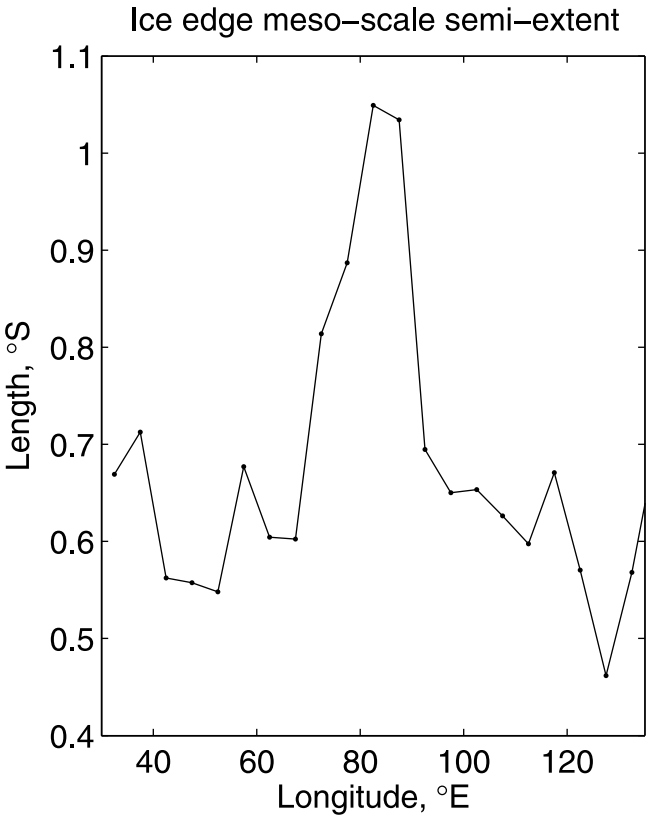

Figure 4. Anomalies of ice edge length, relative to the ice edge smoothed over 1000 km (semiextent, in degrees of latitude). The anomalies are calculated from the 25-year time series of satellite passive microwave data (1978–2004). The sharp peak at 85°E corresponds to the WIST.

RMS ice edge anomaly in this region, which is larger in May and June than in April. However, the interannual variability is large, ranging from a minimum of 0.5° of latitude (in 1989) to a maximum of 3° (in 2002). Figure 7 shows maps of the ice edge for some of these extreme events. The maxima in ice edge anomaly seen in 1984, 1992, 1998 and 2002 (Figure 6) coincide with very prominent ice tongues (Figure 7; ice edge maps are shown in decreasing order of the size of the ice edge anomaly: 2002, 1984, 1992 and 1998). In 1986, 1989 and 1999, the WIST was either not present or weakly developed.

3.3. Why Does a Sea Ice Tongue Form at 85°E?

[15] What is special about 85°E that favors the rapid development of large sea ice tongues in most years (e.g., 20 out of 26 years have RMS ice edge length anomalies greater than one degree of latitude)? We first consider the role of ocean currents. Figure 8 shows the mean dynamic topography at the sea surface relative to 1000 dbar, overlain on the bathymetry. The southern platform of the Kerguelen Plateau, with depths less than 2000 m, provides a significant obstacle to the eastward flow of the Antarctic Circumpolar Current (ACC). Much of the ACC flow, including the southern branch of the Polar Front (SPF) [*Sokolov and Rintoul*, 2007a], passes through the deep gap that bisects the Kerguelen Plateau, the Fawn Trough [*McCartney and Donohue*, 2007; *Roquet et al.*, 2008]. The flow-passing through Fawn Trough includes streamlines that are deflected strongly to the north and west by the obstacle created by the southern Kerguelen Plateau. For example, streamlines found at 63°S upstream of the plateau are forced as far north as 57°S to round the top of the southern Kerguelen Plateau. Once through the Fawn Trough, the flow shifts back to the south. The southernmost streamlines of the ACC pass through the deep channel separating the Kerguelen Plateau from Antarctica, the Princess Elisabeth Trough. After passing through the Trough, the flow turns to the north near 85°E. *McCartney and Donohue* [2007] show that the northward flow along the eastern side of the Kerguelen Plateau is supplemented by a northward flowing western boundary current associated with a strong, largely barotropic, cyclonic gyre in the Australian Antarctic Basin.

[16] The sharp northward turn of the southern streamlines of the ACC occurs near 85°E, the longitude of the WIST, suggesting that sea ice advection by ocean currents plays an important part in the formation of an ice tongue at this location. In Figure 9, a sequence of ice concentration

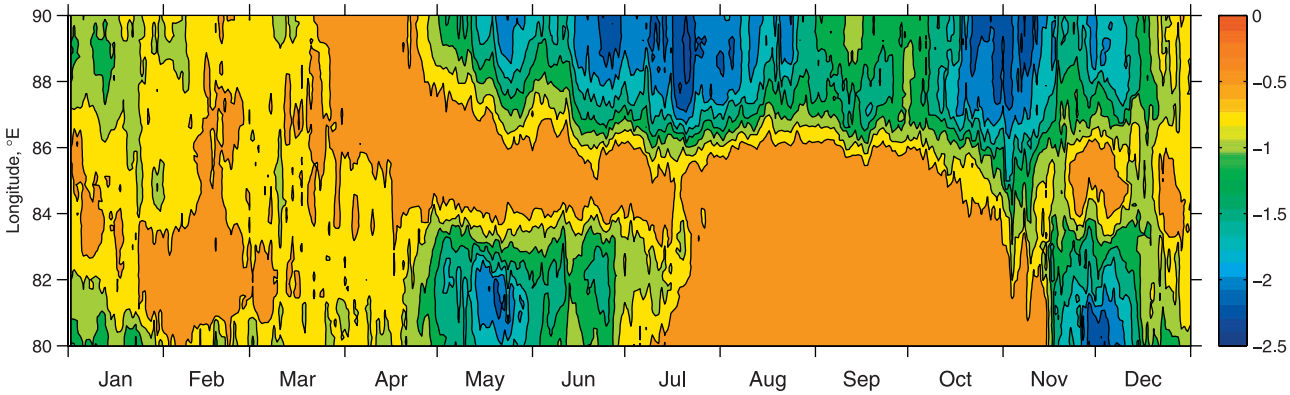

Figure 5. The difference between the latitude of the ice edge at each longitude and the northernmost limit of the ice edge observed between 80° and 90°E (in degrees of latitude), as a function of time. The time series of daily data are averaged over the period between 1997 and 2004. For clarity, contours are not drawn for values greater than −0.5 degrees of latitude. The band of orange values at 85°E flanked by blue between May and July indicates the WIST.

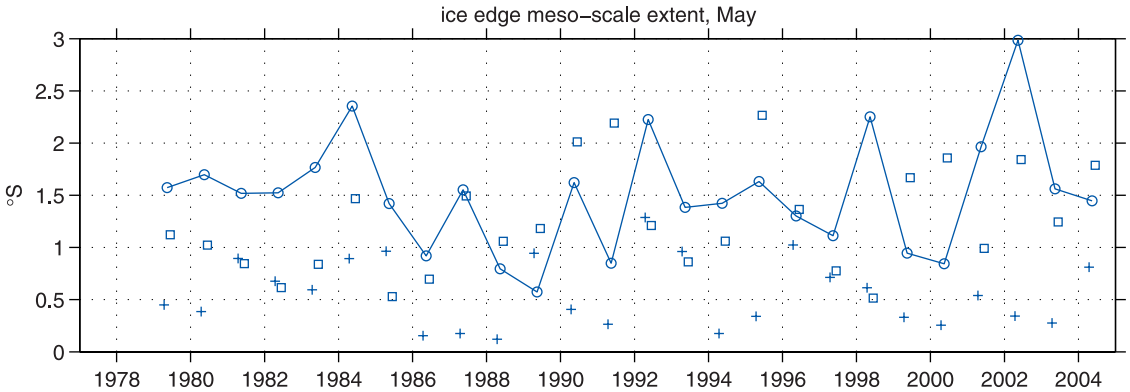

Figure 6. The extent (in degrees of latitude) of ice edge anomalies relative to the ice edge position smoothed over 1000 km scales, for the WIST in May of each year (circles). Extent anomalies for April and June are indicated by pluses and squares, respectively.

images from early April to late May 2002 is overlain on the mean dynamic topography. In early April, the ice edge is relatively zonal, consistent with the more zonal orientation of the streamlines in the southern Princess Elisabeth Trough. The rapid northward expansion of the tongue begins once the ice edge has advanced sufficiently far north (to about 63°S) to reach streamlines that turn sharply to the north. The northward expansion of the tongue seems to stall in mid-May, once the tip of the tongue reaches 60°S, where the northward and southward flows on the eastern side of the Kerguelen plateau converge and turn offshore. As the winter progresses and the sea ice pack continues to expand to the north, the longitude of the maximum sea ice extent shifts slightly to the west (e.g., Figure 3), consistent with the westward bend in the mean dynamic topography (Figure 8). The maximum sea ice extent observed in September–October covers the southern Kerguelen Plateau (Figure 3), bounded to the north by the strong ACC flow-passing through Fawn Trough (Figure 8).

[17] Note that the mean dynamic topography in Figures 8 and 9 is based on relatively scarce data and the streamline pattern is significantly smoothed (e.g., the narrow northward flow on the eastern flank of the southern Kerguelen Plateau [*McCartney and Donohue*, 2007; *Roquet et al.*, 2008] is not well resolved.) high-resolution ocean circulation models show much narrower northward jets on both sides of the Kerguelen Plateau. As an example, we show in Figure 10 some particle trajectories from the OCCAM simulation analyzed by *Thorpe et al.* [2007]. Particles seeded to both the east and west of the Princess Elisabeth Trough are advected strongly offshore in a narrow jet near 85°E. The strong offshore flow at 85°E carries particles seeded near the Antarctic continent as much as 10 degrees of latitude to the north. Only the northward flow on the western flank of the Weddell Sea gyre is of comparable meridional extent. The model suggests the northward flow is fed by inflow from the east at its southern limit, and by inflow from the west further north. Note that the model also clearly shows northward flow rounding both the eastern and western sides of the southern Kerguelen Plateau, north of 60°S. This circulation pattern likely controls the development of the tongue in late winter, when the sea ice reaches its northern limit over the plateau (Figure 3).

[18] The strong currents observed and modeled near 85°E would advect both sea ice and seawater to the north. Currents carrying cold water to the north could assist in the development of an ice tongue by inhibiting melt or encouraging local formation of sea ice. Several pieces of evidence suggest that dynamical processes (i.e., northward advection of sea ice from the south) dominate over thermodynamic processes (i.e.in situ formation of sea ice) in the formation and maintenance of the WIST. The strongest evidence for a dynamical origin comes from observations of sea ice drift [*Fowler*, 2003]. For example, the weekly average sea ice drift vectors in Figure 1c suggest that ice advection was strongly offshore in late May 2002, favoring the development of the WIST. Enhanced offshore drift of sea ice in this region is also clear in monthly mean maps of sea ice drift (Figure 11; the monthly means are computed over the period 1978 to 2003). Strong northward drift occurs near 85°E in May, the period when the WIST grows rapidly at this location. By July, the mean ice edge has reached the southern Kerguelen Plateau and there is strong northward drift between 75°E and 85°E, consistent with the northward bulge of the ice edge over the plateau in July (Figure 4) and the mean dynamic topography (Figure 8). In October, the drift at the ice edge is strongly zonal throughout the region. Once the sea ice extends as far north as the northern limit of the southern Kerguelen Plateau, the strong eastward flow of the ACC carries ice to the east and prevents further northward expansion of the ice tongue.

[19] Strong offshore drift in the vicinity of the WIST can also be inferred by tracking icebergs. A sequence of QuikSCAT images from 10 April to 2 October 2002 shows the drift of two icebergs with initial positions near the West Ice Shelf (Figure 12). While iceberg B moved westward in the Antarctic Coastal Current, iceberg A (further to the north) became incorporated into the WIST and drifted to the N/NW with the surrounding sea ice. Assuming direct courses, the distances travelled by iceberg A in Figure 12 (denoted by arrows) translate to mean daily drift rates of ~4.3 km/day from 10 April to 30 May, ~14.0 km/day from 30 May to 24 June, ~7.8 km/day from 24 June to 13 August, and ~7.7 km/day from 13 August to 2 October, all with a dominant northward component. These are comparable to mean daily iceberg drift rates in the region provided by

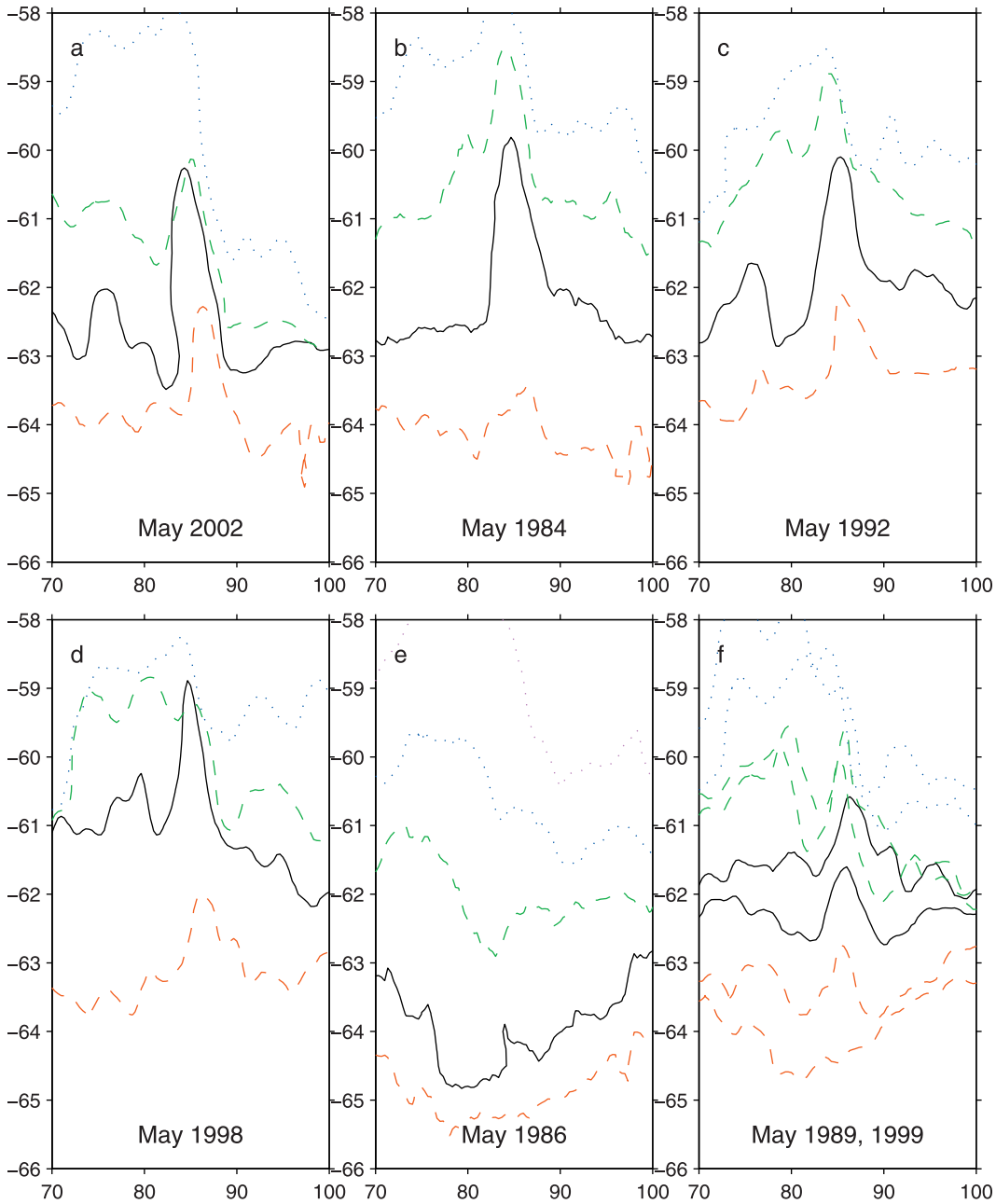

Figure 7. Ice edge positions for years (a) 2002, (b) 1984, (c) 1992, and (d) 1998, corresponding to maximum extent of the WIST. Also shown are ice edge positions for years (e) 1986 and (f) 1989 and 1999, corresponding to minimum extent of the WIST. The ice edge is shown for April (red dashed curve), May (black solid curve), June (green dashed curve), July (blue dotted curve), and August (magenta dotted curve; only present south of 58°S in 1986).

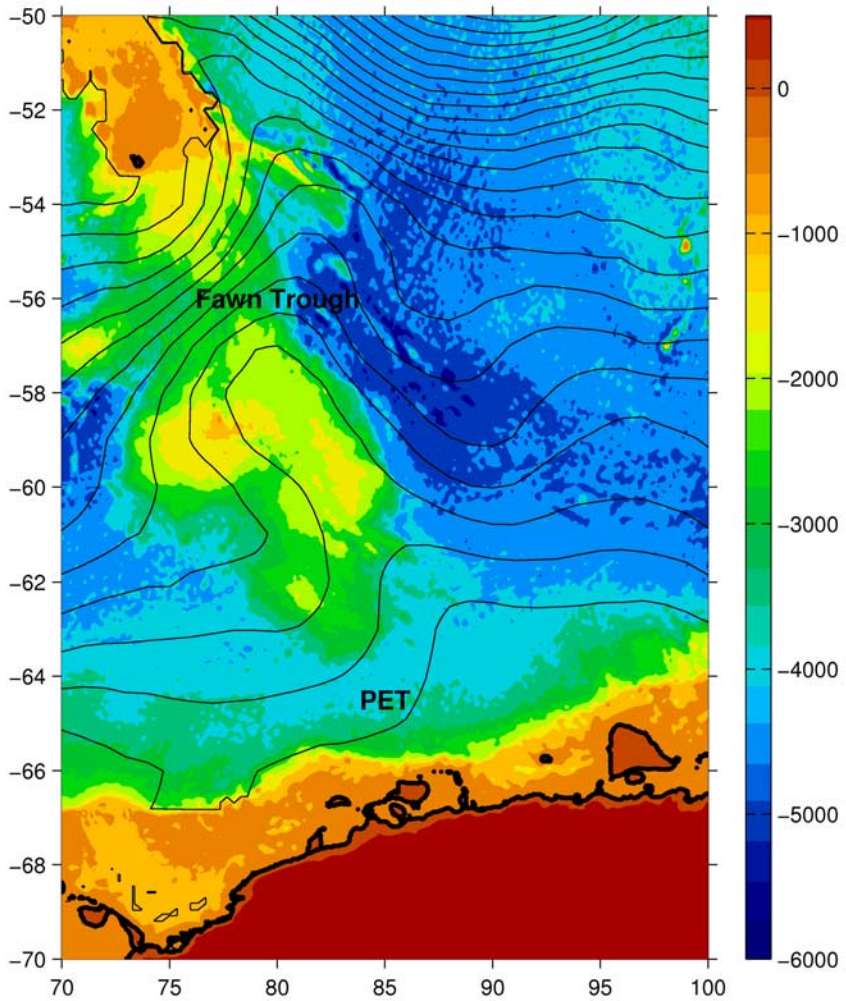

Figure 8. Mean dynamic topography (contours plotted every 2.5 cm relative to 1000 dbar) in the region of the southern Kerguelen Plateau, overlaid on the bathymetry (color). PET, Princess Elisabeth Trough.

Budd [1986], and also sea ice drift rates given by *Heil and Allison* [1999]. Note that iceberg A drifted approximately with the ice edge in late June to early October. Icebergs can be steered by surrounding sea ice when the latter is highly compact and thick e.g., in the perennial sea ice zone of the western Weddell Sea [*Schodlok et al.*, 2006]. In contrast, sea ice in our region of interest is largely divergent and is composed of thinner first year floes, and net iceberg drift is likely to be driven more by ocean currents in the upper 200–400 m of the water column. Given that iceberg A drifted approximately with the ice edge from June through October 2002 (i.e., within the low-concentration marginal ice zone), it is reasonable to conclude that ocean currents carried both the iceberg and the sea ice edge northward during this period; i.e., the northward expansion of the WIST was driven mainly by ice advection (dynamics) rather than ice formation (thermodynamics). Past studies of iceberg drift behavior in the region provide further evidence of a distinct bifurcation in the drift pattern of icebergs passing the West Ice Shelf, with a strong northward retroflection in iceberg drift tracks in the region 80–90°E [*Tchernia and Jeannin*, 1984; *Young and Hyland*, 1997; *Jacka and Giles*, 2007]. Wind-driven sea ice "steering" alone cannot explain this phenomenon, although the latter may be responsible for synoptic-scale deviations (as observed in the central Weddell Sea by *Schodlok et al.* [2006] but unresolved in this study).

[20] A final piece of circumstantial evidence in support of a dynamic origin of the WIST comes from ocean temperature distributions. While there are few observations in winter, especially from within the sea ice pack, it is common to use the temperature of the temperature-minimum layer observed in summer (the so-called Winter Water) to infer the sea surface temperature of the previous winter [e.g., *Park et al.*, 1998]. The temperature-minimum layer in the vicinity of the WIST extends across the Princess Elisabeth Trough and the southern Kerguelen Plateau (e.g., as seen on the potential temperature distribution on World Ocean Circulation Experiment (WOCE) section I8S in the work of *Sparrow et al.* [2005]; see also *Roquet et al.* [2008]). However, temperatures cooler than −1°C are only observed south of 62°S, suggesting either that winter temperatures are

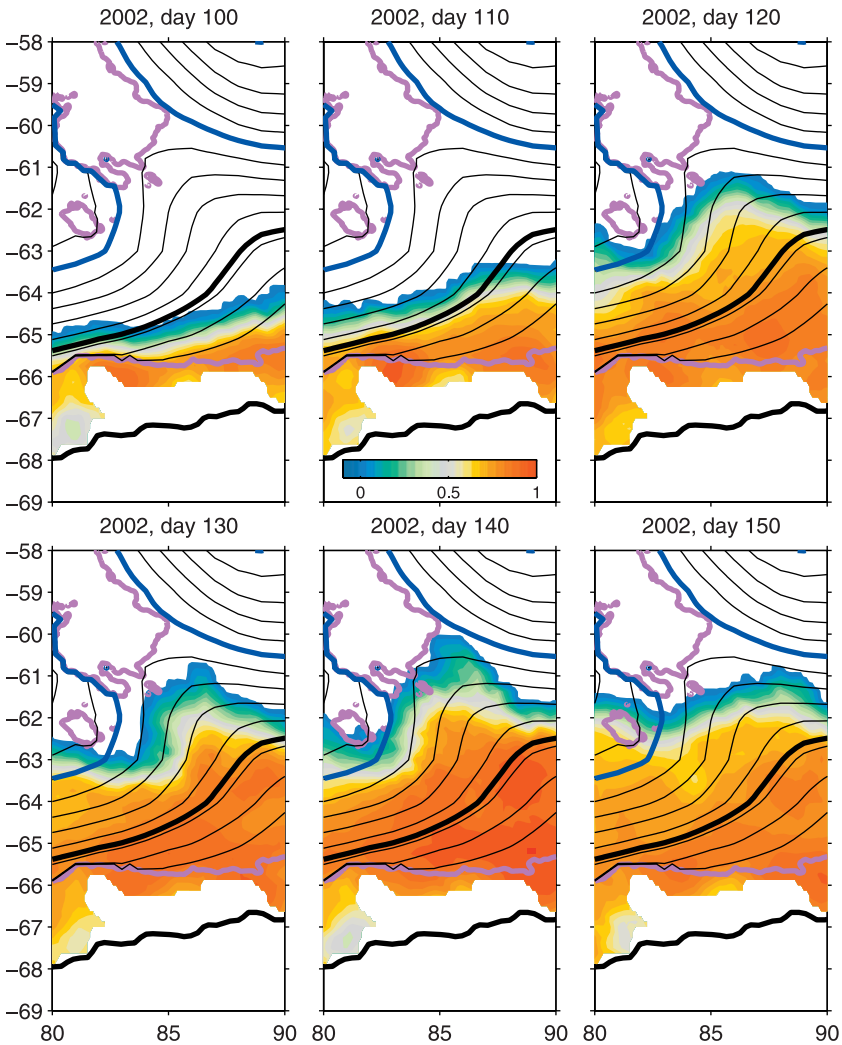

Figure 9. A time sequence of sea ice concentration images illustrating the development of the WIST in 2002 relative to the mean dynamic topography referenced to 2000 dbar and plotted every 2 cm. Positions of the southern boundary of the ACC and the southern branch of the southern ACC front [*Sokolov and Rintoul*, 2007a] are shown by bold black and bold blue curves, respectively. The time series of daily sea ice concentration data are used. The 2000 m bathymetric contour is shown by the magenta bold curve.

too warm for local sea ice formation or that mixing is sufficiently rapid that the temperature-minimum is a poor proxy for winter sea surface temperatures.

[21] Taken together, the sea ice and iceberg drifts and ocean temperatures suggest that the WIST is likely dynamical in origin, although local formation of sea ice may also occur within the WIST. The re-emergence of the WIST as the pack decays in spring may also indicate the importance of advection: while the broad-scale atmospheric and oceanic conditions are conducive to melt, as evident from the rapid retreat of the ice edge to the east and west of the WIST, a supply of ice from the south where conditions remain more favorable for growth may help maintain the WIST. A more definitive conclusion awaits in situ observations of the development and retreat of the sea ice tongue.

3.4. Does the Wind Contribute to the Development of the WIST?

[22] Wind forcing in the region is also favorable for the development of a northward extension of the ice edge in April–May. The meridional component of the mean wind stress in these months is southerly (not shown). Perhaps more revealingly, changes in the strength of the southerly component of the wind appear to be closely related to interannual variability in the magnitude of the WIST. For example, in 2002 and 1984 when large ice tongues were observed (Figure 7), there was a strong northward component to the wind stress anomaly in April, May or both months (where the anomaly is calculated relative to the 26-year mean in each month, Figures 13a–13d). In 1986 and 1989, when the WIST was absent or poorly developed, the meridional component of the wind stress anomaly was weak or southward (Figures 13e–13h).

[23] To further explore the connection between winds and variability of the WIST, we use the singular value decomposition (SVD) to calculate joint EOFs of anomalies in the length of the sea ice edge in May and in May wind stress. The first coupled mode explains 26% of the variance. Figure 14a shows the pattern of sea ice edge variability

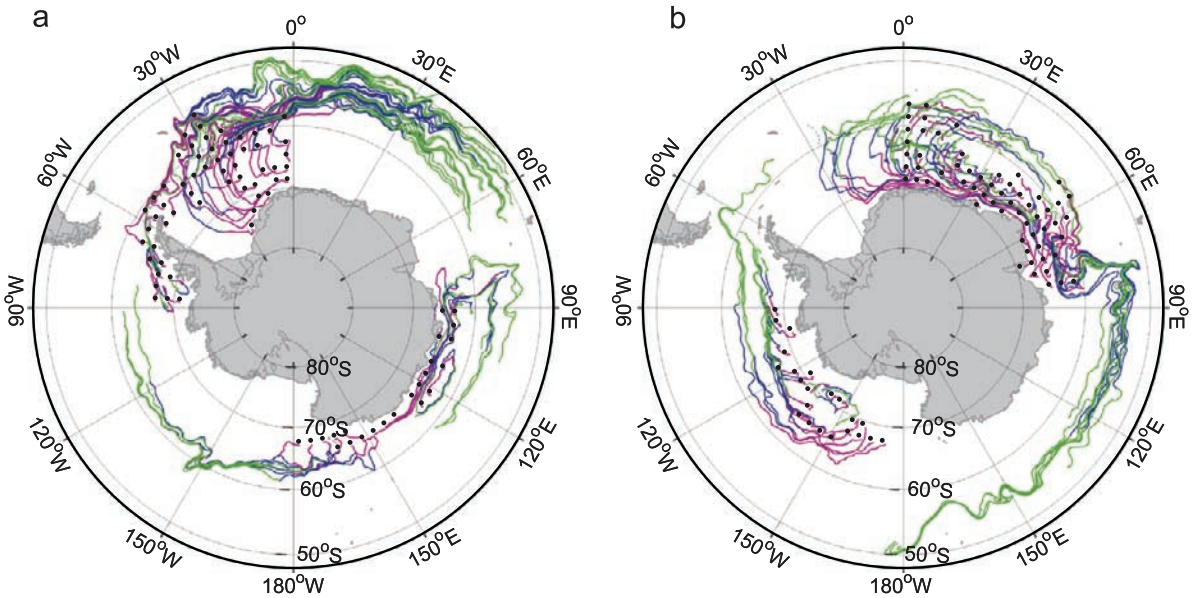

Figure 10. Three-year trajectories of particles computed from output of the OCCAM 1/4° ocean circulation model, plotted according to release regions (a) 90W–0 and 90E–180W and (b) 0–90E and 90W–180 W. The trajectories are derived using combined ocean and sea ice velocity fields (if no ice is present, the particles are advected by the modeled ocean velocity field; if sea ice is present, particles are advected by the ice drift vectors of *Fowler* [2003]). See *Thorpe et al.* [2007] for details. Trajectories are colored according to time: pink, 0–1 year; blue, 1–2 years; green, 2–3 years. Release sites are marked by black dots. Adapted from Figure 4 of *Thorpe et al.* [2007], with permission from Elsevier.

associated with the first coupled mode, which is dominated by a strong peak between 80°E and 90°E corresponding to the WIST. The dominant wind stress pattern associated with the first coupled mode is shown in Figure 14b. A large WIST is associated with southerly winds in the Princess Elisabeth Trough and southeasterly winds further north. Note the strong similarity between the wind stress pattern of the leading coupled mode and the wind stress in May 2002, when the largest WIST was observed (Figure 13b). Figure 14c shows the amplitudes or expansion coefficients associated with the leading mode of sea ice edge and wind stress anomalies. The two time series strongly covary ($r = 0.74$; values greater than 0.49 are significant at the 95% level). In addition, the time series associated with the leading mode is very similar to the time series of ice edge length anomalies (Figure 6). Each of the large positive events in Figure 6 corresponds to a maximum in the EOF time series (e.g., 1984, 1992, 1998, and particularly 2002); each of the large negative anomalies in Figure 6 (e.g., 1986, 1989, 1999–2000) corresponds to large negative values of the amplitudes associated with the wind stress and therefore northerly anomalies.

3.5. Does the WIST Influence Biological Productivity?

[24] Satellite ocean color images reveal that the region of the Kerguelen Plateau and the Princess Elisabeth Trough (PET) has the highest surface chlorophyll values in the Indian and Pacific sectors of the open Southern Ocean (i.e., away from islands and continents) [e.g., *Sokolov and Rintoul*, 2007b]. Several distinct blooms dominate the surface chlorophyll images in the vicinity of the plateau (Figure 15). A large bloom observed to the north and downstream from the northern Kerguelen Plateau has been attributed to natural iron fertilization, with the iron supplied by shallow sedimentary sources on the plateau [*Blain et al.*, 2007]. High chlorophyll is also observed in a more or less continuous band over the Antarctic continental shelf and slope, within or adjacent to the marginal ice zone. Phytoplankton blooms in this region have been attributed to (1) iron supply from shallow sediments and melting sea ice, (2) increased stratification and therefore higher light levels as the result of ice melt in summer, and (3) "seeding" by sea ice algae [e.g., *Smith and Nelson*, 1986].

[25] Elevated surface chlorophyll values are also found over and to the southeast of the southern Kerguelen Plateau. *Sokolov and Rintoul* [2007b] show that the bottom pressure torque resulting from interaction of the ACC with topography drives both the northward currents observed on the flanks of the plateau and upwelling throughout the water column. They argue that this topographic upwelling supplies macronutrients and micronutrients to the euphotic zone, fueling the large phytoplankton blooms observed to occur in the vicinity of major bathymetric features throughout the Southern Ocean. Part of the phytoplankton bloom observed near the southern Kerguelen Plateau is likely supported by this mechanism. However, high-chlorophyll values are also observed over the deep water of the PET, where topographic upwelling would be expected to be weak in the absence of steep topography. The band of high chlorophyll between 85°E and 90°E coincides with the region of strong northward flow responsible for the WIST. It is not clear whether higher biomass is found in this location because the WIST preconditions the area for elevated production in the following summer (through the

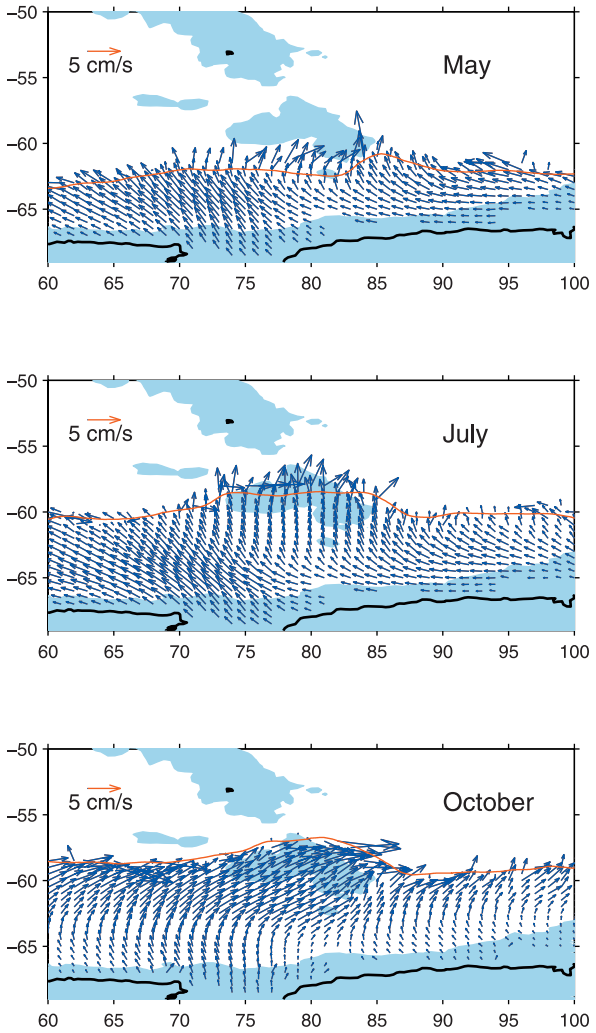

Figure 11. Monthly mean ice motion vectors for May, July, and October averaged over the period between 1978 and 2003. The monthly mean ice edge derived from sea ice concentration images is shown by the red solid line. Depths shallower than 2000 m are shaded.

mechanisms described above for the marginal ice zone) or because currents carry productive waters and biomass offshore from the continental margin bloom (or both). In any case, the bloom over the PET is very persistent. While the blooms downstream of Kerguelen Island and over the Kerguelen Plateau have largely dissipated by February, high surface chlorophyll values are still observed in the PET bloom at that time and relatively high values are still observed there in March (not shown). The fact that both the continental margin and PET blooms persist throughout the summer supports the hypothesis that the PET bloom is supported by advection of biomass and/or nutrients from the south.

4. Discussion

[26] Regional differences in the extent of Antarctic winter sea ice reflect the large-scale circulation of the ocean and atmosphere. For example, extensive winter sea ice occurs in the Weddell and Ross Seas owing to the presence of the major cyclonic gyres, while a narrower sea ice zone is found in regions where the ACC approaches the continent, such as the southeast Indian and Pacific oceans [*Gloersen et al.*, 1992]. At any particular location, the configuration of the ice edge typically responds on timescales of hours to days to changes in winds associated with the passage of storms. Long filaments of ice emerging from the ice edge are often observed, but they are generally ephemeral features that decay as rapidly as they form. Features of comparable area, meridional extent and persistence to the WIST are found nowhere else around the circumpolar Antarctic sea ice zone.

[27] The seasonal progression of the sea ice edge in the vicinity of 85°E illustrates the causes and influence of the WIST. The ice edge is largely zonal at the start of the ice growth period in April (Figure 4). Once the ice edge extends sufficiently far north (~64°S) to reach the middle of the Princess Elisabeth Trough, where the mean streamlines turn to the north, it rapidly expands to the north in a narrow band centered on 85°E. The resulting tongue is most prominent in May, when it extends from the deep water over the trough to the southern edge of the Kerguelen Plateau. During June, the ice edge advances on either side of the WIST, making the tongue become less prominent but still visible in the 26-year mean ice edge for June (Figure 4). As the winter continues, the pack expands further to the north, reaching its maximum extent in September. Throughout the winter, the mean monthly ice edge shows a prominent bulge to the north over the southern Kerguelen Plateau. In other words, the northernmost limit of the pack ice in this sector of the Southern Ocean is found in the vicinity of the WIST throughout the sea ice growth and decay cycle between May and December. The presence of the ice tongue at 85°E maintains sea ice at lower latitudes than observed to the east and west, during both the growth and decay of the sea ice pack.

[28] We have shown that the WIST forms as the result of ocean currents turning sharply to the north around the southeastern edge of the Kerguelen Plateau. The sharp northward turn in this location is supported by bottom pressure torque resulting from interaction of the ACC with the bathymetry along the edge of the plateau [*Rintoul et al.*, 2001; *Sokolov and Rintoul*, 2007b]. This suggests that interactions between the deep-reaching ACC and the topography play a major role in determining the ice extent in this region. The wind field also contributes to the development of an ice tongue, having a southerly component in April–June, when the WIST rapidly expands to the north. Variability in the winds appears to be largely responsible for variations in the meridional extent of the WIST: years of anomalously northerly winds during April–June correspond to years with poorly developed ice tongues, whereas strong and persistent southerlies result in large tongues.

[29] The only somewhat analogous feature to our knowledge occurs in the Arctic, namely, the Odden ice tongue. This large and semirecurrent sea ice promontory forms in the East Greenland Sea and may protrude eastward from the main pack by as much as 5° longitude at about 8°W between 73° and 77°N and can cover 300,000 km^2 [*Shuchman et al.*, 1998; *Wadhams et al.*, 1996]. The Odden differs from the WIST in that it usually forms by thermodynamic (pancake ice formation) rather than dynamic (ice advection) processes (although *Wadhams and Comiso* [1999] note that another

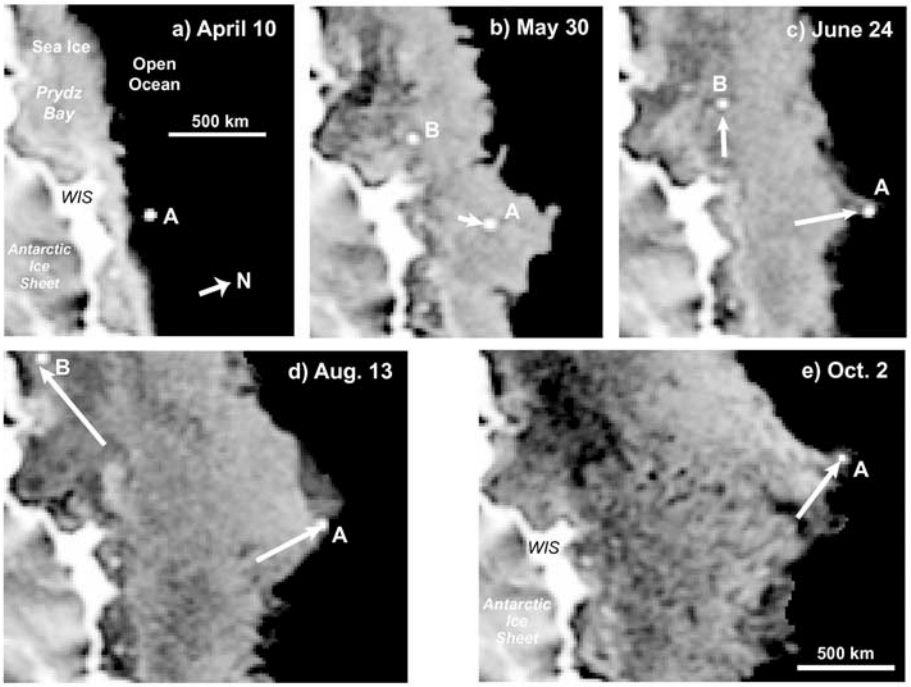

Figure 12. Time series of QuikSCAT enhanced-resolution sigma-0 images of sector 60–95E showing the impact of the WIST on sea ice extent, and the drift of two icebergs (marked A and B), from 10 April to 2 October 2005. WIS, West Ice Shelf. QuikSCAT imagery courtesy of BYU Center for Remote Sensing and NASA.

type of Odden occasionally forms late in the season as the result of advection of old ice originating from the East Greenland Current). The rapid formation and decay of the Odden have been related to both meteorological parameters (air temperature, wind speed and direction) and midgyre ocean convection [*Carsey and Roach*, 1994; *Wadhams et al.*, 1996].

[30] The Odden sea ice cover is believed to play a significant role in the thermohaline circulation in the Greenland Sea, with brine release during sea ice formation driving deep-water convection. The convection ventilates the deep waters of the Greenland Sea, facilitates carbon dioxide sequestration, and helps to drive global thermohaline circulation [*Shuchman et al.*, 1998; *Wadhams et al.*, 1996]. The WIST, being primarily supplied by ice formed in the south rather than by local frazil ice formation, would be expected to supply relatively little brine to the underlying water and in fact no evidence of deep convection has been observed in this region. The net effect of the WIST is likely to cause an increase, rather than a decrease, in stratification, as the result of a net import and melt of sea ice (much as in the case of the "advective" late-season Odden described by *Wadhams and Comiso* [1999]).

[31] Satellite ocean color maps suggest that large and persistent phytoplankton blooms occur in the vicinity of the WIST. Whether productivity is enhanced directly by the WIST (by increasing stratification, nutrient supply or input of sea ice algae to the water column) or by advection of biomass and nutrients by the same current system carrying ice northward (or a combination of the two) is not clear. Several studies indicate that the WIST supports enhanced biological production at higher trophic levels as well. *Tynan* [1997], for example, shows that the distribution of three species of whales was concentrated along the edge of the WIST during a voyage in December 1994. The number of Sperm whales (*Physeter macrocephalus*) caught during the 1950s was more than four times higher between 80° and 90°E than in the 10° longitude sectors to the east and west; catches of Blue whales (*Balaenoptera musculus*) and Humpback whales (*Megaptera novaangliae*) also reached a maximum in the vicinity of the WIST [*Tynan*, 1998; *Mizroch et al.*, 1992; *Holm and Jonsgård*, 1959; *Omura*, 1973]. A summer survey in 1995/1996 between 80°E and 150°E found baleen whales were more common and found at lower latitudes to the west of 105°E [*Thiele et al.*, 2000]. Following *Siegel and Loeb* [1995], *Tynan* [1997] speculated that the sea ice tongue extending to lower latitudes along the eastern flank of the Kerguelen Plateau may support higher densities of krill (*Euphausia superba*). The "Discovery" expeditions [*Marr*, 1962; *Mackintosh*, 1973] and more recent studies [*Nicol et al.*, 2000] indeed found high abundance of krill occurs in the vicinity of the WIST. The model study of *Thorpe et al.* [2007] suggests rapid offshore transport of krill is likely to occur in this region.

[32] During a survey of the region between 80° and 150°E, *Nicol et al.* [2000] found higher concentrations of phytoplankton, krill, whales and seabirds in the west compared to the east. They attributed this spatial contrast to differences in ocean circulation, with an offshore component in the west causing a relatively wide sea ice zone and an onshore flow in the east causing a narrower band of sea ice. Our observations suggest that the offshore flow is in

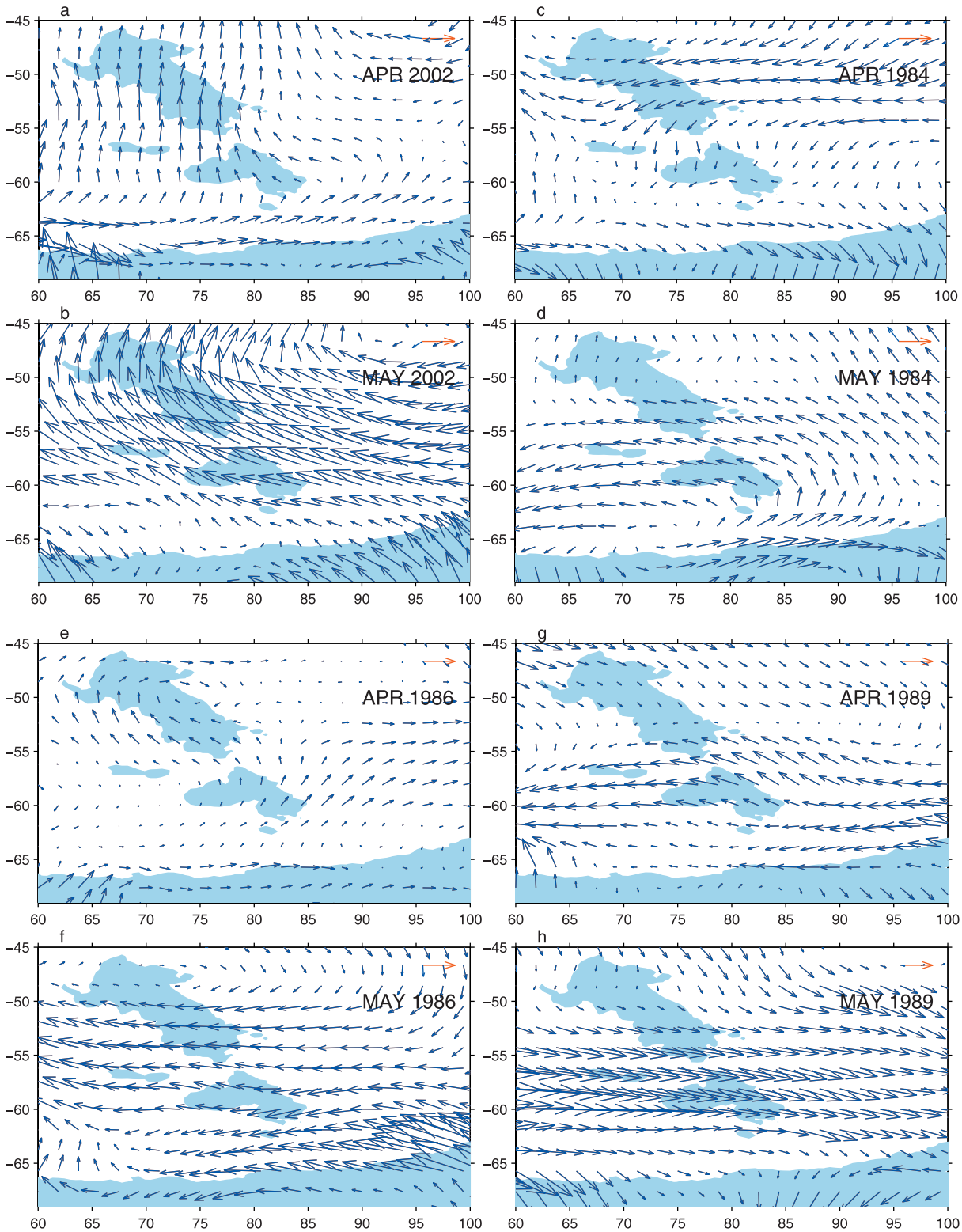

Figure 13. Monthly mean wind stress anomaly from NCEP in April and May for years (a and b) 2002 and (c and d) 1984, of a pronounced WIST, and for years (e and f) 1986 and (g and h) 1989, when the WIST is weak or absent. The anomaly is calculated relative to the mean wind stress for each month calculated from 26 years of reanalysis data. The red scale vector corresponds to 0.1 N m^{-2}. Depths shallower than 2000 m are shaded.

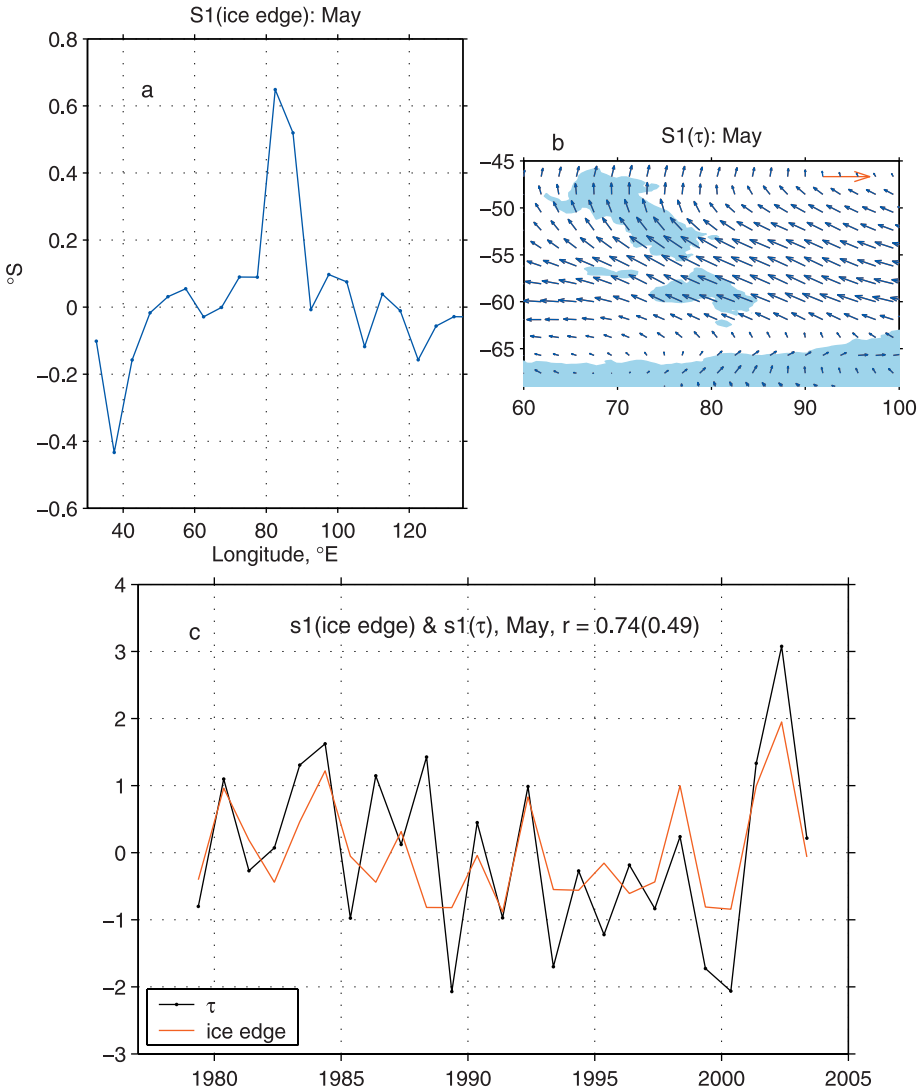

Figure 14. Spatial patterns of (a) extent of ice edge anomalies in May (in degrees of latitude) and (b) monthly mean wind stress anomaly in May of the first joint mode (S1) of the singular value decomposition (SVD). The red scale vector corresponds to 0.1 N m^{-2}. The ice edge anomalies are averaged over five-degree longitude bins; wind stress anomalies are calculated relative to the mean wind stress for May calculated from 26 years of reanalysis data. Depths shallower than 2000 m are shaded. (c) Amplitude time series for the first coupled SVD mode (black is wind stress; red is ice edge). The correlation coefficient r between the two amplitude time series is 0.74; the 95% significance level for the correlation is 0.49.

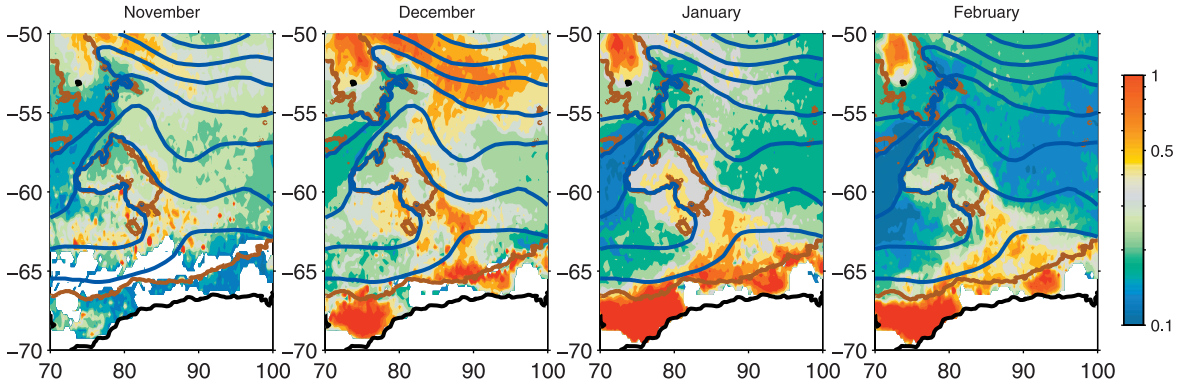

Figure 15. Monthly mean surface chlorophyll (mg/m^3; note logarithmic scale) from SeaWiFS (the mean is calculated for the period 1997 to 2005). Several distinct blooms can be seen in close vicinity to each other: a marginal ice zone bloom in the south, a northern bloom supplied by topographic upwelling, and a bloom over the deep water of the Princess Elisabeth Trough that is coincident with the winter location of the WIST. Mean positions of ACC fronts are shown by bold blue lines. The 2000 m bathymetric contour is indicated by brown bold line.

fact concentrated in a narrow, topographically controlled, jet near 85°E. The strong northward flow along the southeastern flank of the Kerguelen Plateau carries sea ice rapidly to the north to establish the WIST early in the sea ice season. Because the WIST is predominantly made up of ice advected from the south, it may provide a larger source of freshwater during the melt season than the pack ice on either side of the tongue, and therefore support higher biological productivity as well (as a source of iron, algal feed stock, higher stratification, and both habitat and food for krill).

[33] **Acknowledgments.** We thank Tony Worby, Ian Allison, and two anonymous reviewers for their comments on the manuscript. This work is a contribution to CSIRO's Climate Change Research Program and was supported in part by the Australian Government's Cooperative Research Centres Programme through the Antarctic Climate and Ecosystems Cooperative Research Centre. S. R. and S. S. were supported by the CSIRO Wealth From Oceans National Research Flagship. NCEP/NCAR Reanalysis 2 data were acquired from NOAA http://www.cdc.noaa.gov/cdc/reanalysis/reanalysis.shtml. MOA Antarctic coastline and grounding line data, as well as SMMR and SSM/I ice concentration and ice motion data, were obtained from the NASA Earth Observing System Distributed Active Archive Center at the U.S. National Snow and Ice Data Center, University of Colorado, Boulder (http://www.nsidc.org). QuikSCAT data were obtained from NASA's Scatterometer Climate Record Pathfinder data set at Brigham Young University's Center for Remote Sensing. We also wish to thank the SeaWiFS Project (code 970.2) and the Distributed Active Archive Centre (code 902) at the NASA Goddard Space Flight Centre for the production and distribution of the SeaWiFS data, respectively (http://daac.gsfc.nasa.gov/data/dataset/SEAWIFS).

References

Ainley, D. G., and S. S. Jacobs (1981), Seabird affinities for ocean and ice boundaries in the Antarctic, *Deep Sea Res., Part A*, *28*, 1173–1185, doi:10.1016/0198-0149(81)90054-6.

Allen, J. R., and D. G. Long (2006), Microwave observations of daily Antarctic sea-ice edge expansion and contraction rates, *IEEE Geosci. Remote Sens. Lett.*, *3*(1), 54–58, doi:10.1109/LGRS.2005.856710.

Blain, S., et al. (2007), Effect of natural iron fertilization on carbon sequestration in the Southern Ocean, *Nature*, *446*, 1070–1074, doi:10.1038/nature05700.

Bornemann, H., M. Kreyscher, S. Ramdohr, T. Martin, A. Carlini, L. Sellmann, and J. Plotz (2000), Southern elephant seal movements and Antarctic sea ice, *Antarct. Sci.*, *12*, 3–15.

Budd, W. F. (1986), The Southern Hemisphere circulation of atmosphere ocean and sea ice, paper presented at the Second International Conference on Southern Hemisphere Meteorology, Am. Meteorol. Soc., Wellington, New Zealand, 1–5 Dec.

Buesseler, K. O., R. T. Barber, M.-L. Dickson, M. R. Hiscock, J. K. Moore, and R. Sambrotto (2003), The effect of marginal ice-edge dynamics on production and export in the Southern Ocean along 170°W, *Deep Sea Res., Part II*, *50*, 579–603, doi:10.1016/S0967-0645(02)00585-4.

Carsey, F. D., and A. T. Roach (1994), Oceanic convection in the Greenland Sea Odden region as interpreted in satellite data, in *The Polar Oceans and Their Role in Shaping the Global Environment*, *Geophys. Monogr. Ser.*, vol. 85, edited by O. M. Johannessen, R. Muench, and J. E. Overland, pp. 211–222, AGU, Washington, D. C.

Cavalieri, D., C. Parkinson, P. Gloersen, and H. J. Zwally (2006), Sea ice concentrations from Nimbus-7 SMMR and DMSP SSM/I passive microwave data, World Data Cent. for Glaciol. [Snow and Ice], Boulder, Colo.

de la Mare, W. K. (1997), Abrupt mid-twentieth century decline in Antarctic sea ice extent from whaling records, *Nature*, *389*, 57–60, doi:10.1038/37956.

Drinkwater, M. R. (1998), Satellite microwave radar observations of Antarctic sea ice, in *Analysis of SAR Data of the Polar Oceans*, edited by C. Tsatsoulis and R. Kwok, pp. 145–187, Springer, New York.

Early, D. S., and D. G. Long (2001), Image reconstruction and enhanced resolution imaging from irregular samples, *IEEE Trans. Geosci. Remote Sens.*, *39*(2), 291–302, doi:10.1109/36.905237.

Fowler, C. (2003), Polar Pathfinder daily 25 km EASE-grid sea ice motion vectors, World Data Cent. for Glaciol. [Snow and Ice], Boulder, Colo.

Fraser, W. R., and D. G. Ainley (1986), Ice edges and seabird occurrence in Antarctica, *BioScience*, *36*(4), 258–263, doi:10.2307/1310216.

Gloersen, P., W. J. Campbell, D. J. Cavalieri, J. C. Comiso, C. L. Parkinson, and H. J. Zwally (1992), Arctic and Antarctic sea ice, 1978–1987: Satellite passive microwave observations and analysis, *NASA Spec. Publ. SP*, *511*.

Gouretski, V. V., and K. P. Koltermann (2004), WOCE global hydrographic climatology, *Tech. Rep. 35*, Bundesamt für Seeschiffahrt und Hydrogr., Hamburg.

Haran, T., J. Bohlander, T. Scambos, T. Painter, and M. Fahnestock (2006), MODIS mosaic of Antarctica (MOA) image map, World Data Cent. for Glaciol. [Snow and Ice], Boulder, Colo.

Heil, P., and I. Allison (1999), The pattern and variability of Antarctic sea-ice drift in the Indian Ocean and western Pacific sector, *J. Geophys. Res.*, *104*, 15,789–15,802.

Holm, J. L., and Å. Jonsgård (1959), Occurrence of the sperm whale in the Antarctic and the possible influence of the moon, *Norw. Whaling Gaz.*, *4*, 161–182.

Intergovernmental Panel on Climate Change (IPCC) (2007), Summary for policymakers, in *Climate Change 2007: The Physical Science Basis—Contribution of Working Group I to the Fourth Assessment Report of the Intergovernmental Panel on Climate Change*, edited by S. Solomon et al., pp. 1–18, Cambridge Univ. Press, New York.

Jacka, T. H., and A. B. Giles (2007), Antarctic iceberg distribution and dissolution from ship-based observations, *J. Glaciol.*, *53*(182), 341–356, doi:10.3189/002214307783258521.

Kalnay, E., et al. (1996), The NCEP-NCAR 40-year reanalysis project, *Bull. Am. Meteorol. Soc.*, *77*, 437–471, doi:10.1175/1520-0477(1996)077<0437:TNYRP>2.0.CO;2.

Le Traon, P., F. Nadal, and N. Ducet (1998), An improved mapping method of multisatellite altimeter data, *J. Atmos. Oceanic Technol.*, *15*, 522–534, doi:10.1175/1520-0426(1998)015<0522:AIMMOM>2.0.CO;2.

Lubin, D., and R. A. Massom (2006), *Polar Remote Sensing*, vol. 1, *Atmosphere and Polar Oceans*, 756 pp., Springer, New York.

Mackintosh, N. A. (1973), Distribution of post-larval krill in the Antarctic, *Discovery Rep.*, *36*, 1–94.

Marr, J. W. S. (1962), The natural history and geography of the Antarctic krill (*Euphausia superba*), *Discovery Rep.*, *32*, 33–464.

Massom, R. (1992), Observing the advection of sea ice in the Weddell Sea using buoy and satellite passive microwave data, *J. Geophys. Res.*, *97*, 15,559–15,572.

McCartney, M. S., and K. A. Donohue (2007), A deep cyclonic gyre in the Australian-Antarctic Basin, *Prog. Oceanogr.*, *75*, 675–750, doi:10.1016/j.pocean.2007.02.008.

McClain, C. R., M. L. Cleave, G. C. Feldman, W. W. Gregg, S. B. Hooker, and N. Kuring (1998), Science quality SeaWiFS data for global biosphere research, *Sea Technol.*, *39*, 10–16.

Mizroch, S. A., D. W. Rice, and S. W. Larson (1992), Distribution of rorquals in the Southern Ocean: An atlas based on pelagic catch data, *Int. Whaling Comm. Sci. Rep.*, *SC/44/SHB 17*, Int. Whaling Comm., Cambridge, U. K.

Nicol, S., T. Pauly, N. L. Bindoff, S. Wright, D. Thiele, G. W. Hosie, P. G. Strutton, and E. Woehler (2000), Ocean circulation off East Antarctica affects ecosystem structure and sea-ice extent, *Nature*, *406*, 504–507, doi:10.1038/35020053.

Omura, H. (1973), A review of pelagic whaling operations in the Antarctic based on the effort and catch data in 10° squares of latitude and longitude, *Sci. Rep. Whales Res. Inst.*, *25*, 105–203.

Park, Y. H., E. Charriaud, and M. Fieux (1998), Thermohaline structure of the Antarctic Surface Water/Winter Water in the Indian sector of the Southern Ocean, *J. Mar. Syst.*, *17*, 5–23, doi:10.1016/S0924-7963(98)00026-8.

Remund, Q. P., D. G. Long, and M. R. Drinkwater (2000), An iterative approach to multisensor sea ice classification, *IEEE Trans. Geosci. Remote Sens.*, *38*(4), 1843–1856, doi:10.1109/36.851768.

Ribic, C. A., D. G. Ainley, and W. R. Fraser (1991), Habitat selection by marine mammals in the marginal ice zone, *Antarct. Sci.*, *3*, 181–186, doi:10.1017/S0954102091000214.

Rintoul, S. R., C. Hughes, and D. Olbers (2001), The Antarctic Circumpolar System, in *Ocean Circulation and Climate*, edited by G. Siedler, J. Church, and J. Gould, pp. 271–302, Elsevier, New York.

Roquet, F., Y.-H. Park, C. Guinet, and J.-B. Charrassin (2008), Observations of the Fawn Trough Current over the Kerguelen Plateau using data derived from instrumented elephant seals, *J. Mar. Syst.*, in press.

Sarmiento, J. L., and C. Le Quéré (1996), Oceanic carbon dioxide uptake in a model of century-scale global warming, *Science*, *274*, 1346–1350, doi:10.1126/science.274.5291.1346.

Savage, G., J. Priddle, L. C. Gilpin, U. Bathmann, E. J. Murphy, N. J. P. Owens, R. T. Pollard, D. R. Turner, C. Veth, and P. Boyd (1996), An assessment of the role of the marginal ice zone in the carbon cycle of the Southern Ocean, *Antarct. Sci.*, *8*, 349–358.

Schodlok, M. P., H. H. Hellmer, G. Rohardt, and E. Fahrbach (2006), Weddell Sea iceberg drift: Five years of observations, *J. Geophys. Res.*, *111*, C06018, doi:10.1029/2004JC002661.

Shuchman, R. A., E. G. Josberger, C. A. Russel, K. W. Fischer, O. M. Johannessen, J. Johannessen, and P. Gloersen (1998), Greenland Sea Odden sea ice feature: Intra-annual and interannual variability, *J. Geophys. Res.*, *103*, 12,709–12,724.

Siegel, V., and V. J. Loeb (1995), Recruitment of Antarctic krill (Euphausia superba) and possible causes for its variability, *Mar. Ecol. Prog. Ser.*, *123*, 45–56, doi:10.3354/meps123045.

Siniff, D. B. (1991), An overview of the ecology of Antarctic seals, *Am. Zool.*, *31*, 143–149.

Smith, W. O., Jr., and D. M. Nelson (1986), Importance of ice edge phytoplankton production in the Southern Ocean, *BioScience*, *36*, 251–257, doi:10.2307/1310215.

Sparrow, M., P. Chapman, and J. Gould (Eds.) (2005), *Hydrographic Atlas of the World Ocean Circulation Experiment*, vol. 1, *Southern Ocean*, Int. WOCE Proj. Off., Southampton, UK.

Sokolov, S., and S. R. Rintoul (2002), The structure of Southern Ocean fronts at 140°E, *J. Mar. Syst.*, *37*, 151–184, doi:10.1016/S0924-7963(02)00200-2.

Sokolov, S., and S. R. Rintoul (2007a), Multiple jets of the Antarctic Circumpolar Current south of Australia, *J. Phys. Oceanogr.*, *37*, 1394–1412, doi:10.1175/JPO3111.1.

Sokolov, S., and S. R. Rintoul (2007b), On the relationship between fronts of the Antarctic Circumpolar Current and surface chlorophyll concentrations in the Southern Ocean, *J. Geophys. Res.*, *112*, C07030, doi:10.1029/2006JC004072.

Squire, V. A. (1998), The marginal ice zone, in *Physics of Ice-Covered Seas*, vol. 1, edited by M. Leppäranta, pp. 381–446, Helsinki Univ. Press, Helsinki.

Tchernia, T., and T. F. Jeannin (1984), Circulation in Antarctic waters as revealed by iceberg tracks 1972–1983, *Polar Rec.*, *22*(138), 263–269.

Thiele, D., and P. C. Gill (1999), Cetacean observations during a winter voyage into Antarctic sea ice south of Australia, *Antarct. Sci.*, *11*, 48–53, doi:10.1017/S0954102099000073.

Thiele, D., E. T. Chester, and P. C. Gill (2000), Cetacean distribution off eastern Antarctica (80–150°E) during the Austral summer of 1995/1996, *Deep Sea Res. Part II*, *47*, 2543–2572.

Thorpe, S. E., E. J. Murphy, and J. L. Watkins (2007), Circumpolar connections between Antarctic krill (*Euphausia superba* Dana) populations: Investigating the roles of ocean and sea ice transport, *Deep Sea Res., Part I*, *54*, 792–810, doi:10.1016/j.dsr.2007.01.008.

Tynan, C. T. (1997), Cetacean distributions and oceanographic features near the Kerguelen Plateau, *Geophys. Res. Lett.*, *24*, 2793–2796.

Tynan, C. T. (1998), Ecological importance of the southern boundary of the Antarctic Circumpolar Current, *Nature*, *392*, 708–710, doi:10.1038/33675.

Wadhams, P., and J. C. Comiso (1999), Two modes of appearance of the Odden ice tongue in the Greenland Sea, *Geophys. Res. Lett.*, *26*, 2497–2500.

Wadhams, P., J. C. Comiso, E. Prussen, S. Wells, M. Brandon, E. Aldworth, T. Viehoff, R. Allegrino, and D. R. Crane (1996), The development of the Odden ice tongue in the Greenland Sea during winter 1993 from remote sensing and field observations, *J. Geophys. Res.*, *101*, 18,213–18,236.

Young, N. W., and G. Hyland (1997), Applications of time series of microwave backscatter over the Antarctic region, *Eur. Space Agency Spec. Publ.*, *ESA SP 414*, 1007–1014.

R. A. Massom, Australian Antarctic Division, Antarctic Climate and Ecosystems Cooperative Research Centre, Private Bag 80, Hobart, Tasmania 7001, Australia.

S. R. Rintoul and S. Sokolov, Centre for Australian Weather and Climate Research, GPO Box 1538, Castray Esplanade, Hobart, Tasmania 7001, Australia. (steve.rintoul@csiro.au)